*the*s*is*

Ing. Prokop Moravec

Shape Optimization of the Hydraulic Machine Flow Passages

SHAPE OPTIMIZATION OF THE HYDRAULIC MACHINE FLOW PASSAGES

TVAROVÁ OPTIMALIZACE PRŮTOČNÝCH ČÁSTÍ HYDRAULICKÝCH STROJŮ

ZKRÁCENÁ VERZE PH.D. THESIS

Keywords:

Shape optimization, CFD, Particle swarm optimization, PSO, Multi-objective particle swarm optimization, MOPSO, pump impeller, pump turbine, low specific speed pump, Nelder-Mead.

Klíčová slova:

Tvarová optimalizace, CFD, Particle swarm optimization, PSO, Multi-objective particle swarm optimization, MOPSO, oběžné kolo čerpadla, čerpadlová turbína, čerpadlo s nízkými specifickými otáčkami, Nelder-Mead.

Místo uložení práce

Areálová knihovna. Vysoké učení technické v Brně, Fakulta strojního inženýrství.

CONTENT

INTRODUCTION

A well-known technical problem called a **shape optimization** has become increasingly popular amongst engineers in various parts of industry or academia in the past few years, primarily thanks to a development of computer technology and a specialized software connected with it. The main goal of every shape optimization process is to provide a shape/size (we can call it **design**) that fulfils given parameters and satisfies chosen constraints.

Authors in [14] suggest that the final design must be as good as possible in some defined sense, but for a lot of optimization problems is sufficient any feasible improvement of the initial shape - this approach is for our purposes quite adequate and also reasonable. Presented work focuses its full energy mainly on the shape optimization in a field of the hydraulic machinery - to be more accurate in a field of the centrifugal radial pumps. The key question of finding the optimal design of a certain flow part strongly relies on two crucial things: **first** on an accurate numerical simulation of the current flow via Computational Fluid Dynamics (CFD) and **second** on a suitable choice of a proper optimization method or approach. But it must be noted that not every combination of these two prerequisites is a win situation, they must be carefully merged in the most effective way - in terms of a minimizing of a total computational time due to a time-consuming nature of CFD simulations.

The pivotal aim of this work is set to explore a **Particle swarm optimization algorithm** (shortly PSOA) and its possible modifications to create an **optimization tool** for designing a proper shape of chosen radial pump impellers. PSOA is extensively influenced by the social behaviour of miscellaneous animals, such as birds, fish, etc. This method shows convenient and perspective attributes, that could be utilized in the shape optimization of the chosen flow parts in hydraulic machinery, mostly: could be effectively programmed (the PSOA is defined by two basic equations - velocity and position calculations), a great robustness of an optimization search ability (due to a stochastic nature of the algorithm) or an option to a possible computational parallelization (each particle could be investigated separately during one iteration of the algorithm). And together with **Pareto principles**, the Particle swarm optimization algorithm could be successfully used in multi-objective shape optimization problems.

The shape optimization tool was applied on a problem of finding the proper **pump turbine** design (grant **TH01020982** - *Zefektivnění akumulace energie a zajištění stability rozvodné sítě rozšířením provozního pásma přečerpávacích vodních elektráren*). This design is supported with both, CFD simulations and with an experiment performed by ČKD Blansko Engineering. Another task, which served as a test case for the future optimization tool, was a problem of finding the proper shape of the very **low specific speed centrifugal pump** [6], [7].

1 THEORY

This chapter covers a mathematical basis around the chosen Multi-objective PSO method, which was used in the impeller shape optimization procedure.

1.1 Multi-objective particle swarm optimization

Multi-objective particle swarm optimization uses Pareto principles to locate proper optimum of the evaluated problem [2], [3].

1.1.1 Main algorithm

The fundamental movement of particles for Multi-objective particle swarm optimization (shortly MOPSO) is captured by equation [3]:

$$v_{in} = w \cdot v_{in} + c_1 \cdot rand() \cdot (p_{in} - x_{in}) + c_2 \cdot Rand() \cdot (rep_n - x_{in}), \tag{1.1}$$

where c_1 and c_2 are positive constants; w is inertia weight, $rand()$ and $Rand()$ are two random vectors from range (0, 1); v_{in} is the velocity (step size) of the $\overline{ith}$ particle; x_{in} is a current position of the ith particle; p_{in} is the best previous position of the $\overline{ith}$ particle (personal best); rep_n is a leader particle selected from an external archive. Particle positions are afterwards computed by rule [3]:

$$x_{in} = x_{in} + v_{in}. \tag{1.2}$$

External archive
The major task of the external archive (repository) is to keep records of the nondominated solutions, which were found during the optimization cycle [3]. The external repository consists of two main parts: the repository controller and the grid [3].

Repository controller [3]: The controller decides, when a certain solution is suitable for archive or not. Solutions, which are not dominated, are each iteration of the algorithm compared against solutions, which are already stored in external depository. The archive is empty at first, so current solution is accepted at the beginning of the algorithm (case 1 in fig. 1.1). If some new solution is dominated by some member from the external archive, then this solution is automatically discarded (case 2 in fig. 1.1). On the other hand, if none of the solutions stored in the external repository dominates the new solution, then the new solution is placed into the archive (case 3 in fig. 1.1). If there are solutions in the archive that are dominated by the new solution, then these solutions are deleted from the repository (cases 4 in fig. 1.1). Ultimately, if the external archive is full, the adaptive grid procedure must take place (case 5 in fig. 1.1) [3].
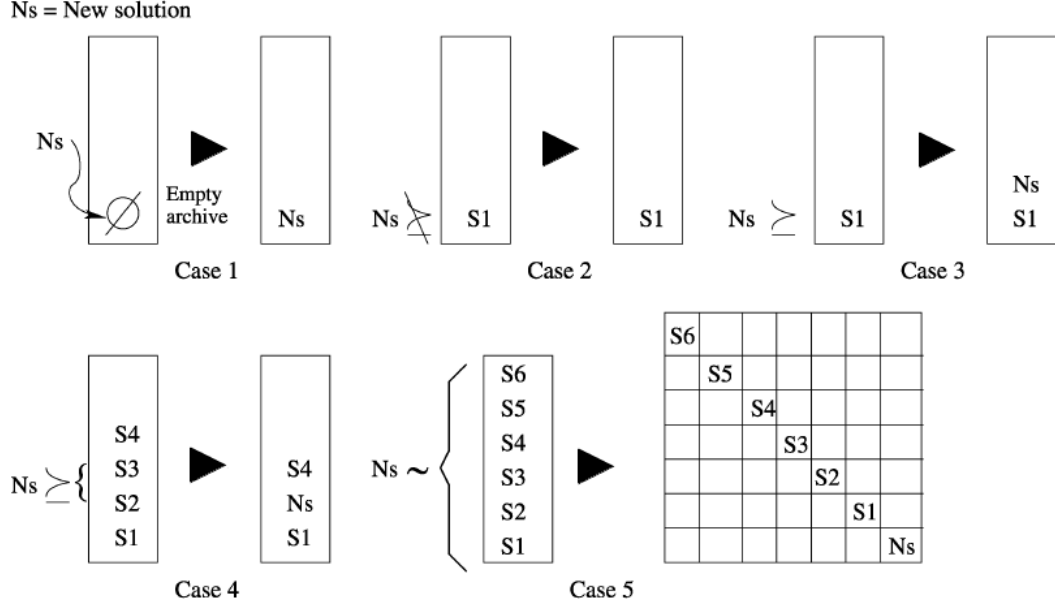
Fig. 1.1*: Archive cases* [3].

Adaptive grid [3]: The grid maintains well-distributed Pareto front - serves in selection of a particle leader and later in a deletion of redundant particles in archive. Simple grid of a constant number of nodes always encloses particles in external archive. This enclosed area is divided by the grid into several rectangle sub areas. Each sub areas with particle(s) are provided by a chosen weight factor. Value of the weight factor is set according to the next algorithm procedure - leader selection or particle deletion.

Leader $\mathbf{rep_n}$ selection [3]: Leader $\mathbf{rep_n}$ is chosen from external repository by a roulette-wheel selection. Every sub area with a particle(s) is provided with the weight factor - sub areas with one particle have greater weight values compared to sub areas with multiple particles.

Particle deletion [3]: Redundant particles are deleted by similar principle, which was used in the leader selection. Sub areas with multiple particles has greater weight factor compared to sub areas with only one particle.

Roulette wheel selection [3]: Roulette wheel selection assigns probability values proportional to a fitness of each individual (particle, design). After that, roulette selects from such distribution - fit individuals get a better chance of being selected, on the other hand less-fit individuals get lower chances. Fitness of each particle is calculated according to chosen function, which will be described in section 2 called *Shape optimization procedure.* The main task of roulette wheel selection is to maintain diversity of the optimization procedure (avoid premature swarm convergence).

2 SHAPE OPTIMIZATION PROCEDURE

The presented shape optimization tool will find its most suitable application in the area of the **centrifugal radial pump** impellers.

2.1 Master code

Under a concept of the **master code** are hidden lines of a very complex code, compiled within Matlab programming language (using free licence software GNU Octave), which has the significant role in the shape optimization algorithm. This code calls and handles the MOPSO algorithm, which is described in sec. 2.1.2, an impeller modeller mentioned in sec. 2.1.3, a mesh generator characterized in sec. 2.1.4 and a CFD solver remarked in sec. 2.1.5. Every software in all these steps works in a so-called **batch mode** - a software run in a Windows/Linux background without any graphical user interface. This run is handled via text scripts, which are in more detail described in following sections.

2.1.1 Software input

It must be noted, that the optimization algorithm needs some initial design to begin with. This starting 1D design is based on the empirical relations found in [4], [5], [10]. The optimization software requires namely: main four points in R-z coordinate system, which characterize the size and position of the meridional flow channel; the number of blades **z** [-], the blade thickness Δ [mm] on the three main streamlines (hub, middle, shroud); the requested head **H** [m]; the requested flow rate **Q** [m^3/s] and the requested rotational speed (RPM) **n** [1/min].

Another important input parameter is the reasonable choice of the pump's operational range. Customers want in many occasions to have guaranteed pump operational range with the highest possible efficiency together with required head.

The crucial dimensions, which are computed by the optimization software (based on the empirical study [4], [5], [10]) are β_1 [°] angle of the blade at inlet, β_2 [°] angle of the blade at outlet and the diameter d_1 [mm]. It must be noted that the diameter d_1 served only for the determination of β_1 angle and did not have another job in the shape optimization procedure.

2.1.2 MOPSO

A leading role of the optimization cycle is proper optimization method. In this case the MOPSO (in more detail described in sec. 1.1) with Pareto principles and several modifications was utilized in the problem of designing the proper shape of the pump impeller.

Optimization objectives and evaluation function
Every optimization method or algorithm is driven by a chosen optimization objective(s). In the presented shape optimization procedure are chosen these: the hydraulic efficiency

η_H, the pump head H and the static relative pressure on the blade. These three objectives together with shape penalties, which ensure the creation of suitable designs, formed the **evaluation function** f. The main task of the function f and its **minimal** value is to select the "best" design from the external archive (the best in the meaning of what is the best for the user and his parameter input).

$$f = weight_H \cdot \left| 1 - \frac{H_{opt}}{H_{req}/const_H} \right| + weight_\eta \cdot (3 - \eta_{H,-} - \eta_{H,opt} - \eta_{H,+}) +$$
$$+ weight_{surf} \cdot (1 - C_{pressure}) + pen_{shroud} + pen_{hub} + 0.2 \cdot pen_\theta + pen_{HQ}, \quad (2.1)$$

where H_{opt} $[m]$ is the current value of pump head acquired from CFD; $\eta_{H,-}$ $[-]$ is the hydraulic efficiency acquired from CFD in the operating point on the left from pump optimum; $\eta_{H,opt}$ $[-]$ is the hydraulic efficiency acquired from CFD in the pump optimum; $\eta_{H,+}$ $[-]$ is the hydraulic efficiency acquired from CFD in the operating point on the right from the pump optimum. The rest of the variables are described in a following text.

Weights $weight_H$, $weight_\eta$ and $weight_{surf}$: A magnitude of each weight sets a partial goal in the optimization procedure. For example with the higher value of the $weight_H$ is swarm strongly influenced by the change of the pump head H, on the other hand remaining objectives are suppressed.

Constant $const_H$: The presented optimization procedure uses only one periodical flow channel, which means that the additional parts of pump such as the diffuser, volute or distributor are neglected. The fluid, which passes through the neglected parts, is affected by losses. These losses decrease value of the pump head and efficiency, so to balance this problem, requested value of the pump head must be boosted by a chosen constant $const_H = \mathbf{0.975}$. Such value is based on the research in [1], where authors determined the difference between the head of the impeller and the head of the impeller with the volute to approximately 3%.

Variable $C_{pressure}$: The blade experiences the low pressure states on its suction side, so from this perspective the blade must be checked for the critical values of this pressure for a possible manifestation of the cavitation. Thus, the variable $C_{pressure}$ $[-]$ is defined as a ratio between the area of the blade $S_{pressure}$ $[m^2]$ with the static relative pressure equal and lower than a chosen value $(-\ 75000\ Pa)$ and the total area of the blade S_{blade} $[m^2]$. It must be noted that the variable/penalty $C_{pressure}$ $[-]$ does not necessary exclude the pump designs with the low values of the static pressure on the blade, it only penalizes them significantly.

Penalties pen_{hub} and pen_{shroud}: A key role of the penalties pen_{hub} and pen_{shroud} is to penalize the deformed shapes of the Bézier curves, which are the foundations of the hub and the shroud of the centrifugal pump impeller.

Penalty pen_θ: Another type of the computational penalty must be set to avoid the creation

of the deformed blade shapes at the impeller outlet (trailing edge deformation) - pen_θ. Such trailing edge deformations make usually the hydraulic design unmanufacturable.

Penalty pen_{HQ}: A key role of this penalty is to penalize the pump impeller designs, which create a H-Q instability in the chosen working range. It means that, if the head value in the operating point on the left from the optimal flow rate has the smaller value than in the optimal flow rate, the current design shows signs of the instability. This penalty has only two values: if the instability is present $pen_{HQ} = \mathbf{1}$, otherwise $pen_{HQ} = \mathbf{0}$.

Nelder-Mead modification and swarm diversity restart

An idea of a combination of two optimization algorithms (**Particle Swarm Optimization**, **Nelder-Mead algorithm**) was explored in [9]. This idea was transformed and modified into this optimization procedure and afterwards applied on the key element of the MOPSO algorithm - on the external archive, where Pareto dominant designs are stored.

A final improvement of the swarm diversity is by a so called "**restarting**" of the current swarm (could be compared to the mutation mentioned above in the MOPSO section, which is plentifully exploited in EA/GA). A restart concept is defined as a creation of the completely new swarm with random parameters (identical procedure takes place at the beginning of MOPSO algorithm). But it must be noted that this restart procedure does **NOT** replace current swarm at all cost, just only if a newly restarted particle improves the current one. This procedure takes place every **third** iteration of the MOPSO algorithm.

Two types of swarm restart are implemented inside the optimization algorithm and while iteration goes on, they'll alternate between each other. **First** restart utilizing the whole given computational areas for changing parameters. **Second** restart is based on the knowledge from [4], which utilizes the inflection points in β angle developments.

2.1.3 Parametric model

The most effective way, how to create a specific design of the centrifugal radial pump impeller, is by using the commercial ANSYS software package with a specialized tool **BladeGen**. BladeGen (running in the batch mode) could be controlled via a text script file *.bgi*. The crucial parameters of the pump impeller could be defined in such file, namely: β - the angle of the blade (inlet/outlet angles); the blade thickness; the shape of a meridional flow channel (with the Bézier curves or splines) or the position of a leading edge and its form. The shape of each impeller is in the presented thesis (optimization tool) parametrized in three main steps: the meridional parametrization, the blade parametrization and the leading edge parametrization. It must be noted that the operating limits (boundaries) of the parametric model are **first** developed around data from empirical equations and later during the optimization run around the best suitable design proposed by the function f (see equation 2.1) $\rightarrow$ the floating operational boundaries.

2.1.4   Computational mesh

The mesh generation is ensured by a tool called **TurboGrid** (also belongs in the commercial ANSYS product package). TurboGrid excels in the meshes for rotational machines and it is tightly connected with the **BladeGen** output. This software is also handled and managed by a text script file called **replay** (basically, replay is a simple record of actions, which were executed during the mesh creation in TurboGrid). One periodical flow channel was used, with hexahedral elements and higher mesh resolution near walls. Total element count did not exceed **250k cells**.

Negative volume detection
Important step in presented computational hierarchy is a procedure called **negative volume detection**, which is performed by **ICEM CFD**. This procedure takes place right after the generation of the computational mesh and has a task of revealing deformed mesh cells inside the computational domains, which are afterwards discarded.

2.1.5   CFD simulation

A proper CFD simulations were handled via commercial software **ANSYS CFX**. ANSYS CFX stands out in the area of CFD simulations connected with the rotational hydraulic machines like pumps, turbines etc. Every numerical calculation was performed as a **steady** simulation with a periodical flow channel and with a frozen rotor model used on interfaces, which connected static and rotational domains. As boundary conditions served a zero static relative pressure at the domain inlet and a constant mass flow at the outlet. It must be noted that CFD simulations were performed for three different mass flows, which corresponded with the working operational range set by the user at the beginning of the optimization cycle.

Computational parallelization
One of the most important advantage of PSO (MOPSO) algorithm is that the necessary CFD simulations could be redistributed to multiple workers. This fact is transformed into a batch calculation using a department cluster called **KAPLAN** and a simple **shell** script file - it means that the all designs are sent for the CFD simulations at once → significant savings in the total computational time.

3 TOOL APPLICATION

Presented optimization software, which employs MOPSO and NM algorithms and procedures, possesses an output graphical interface, which is divided into the five pump property windows - described by fig. 3.1.
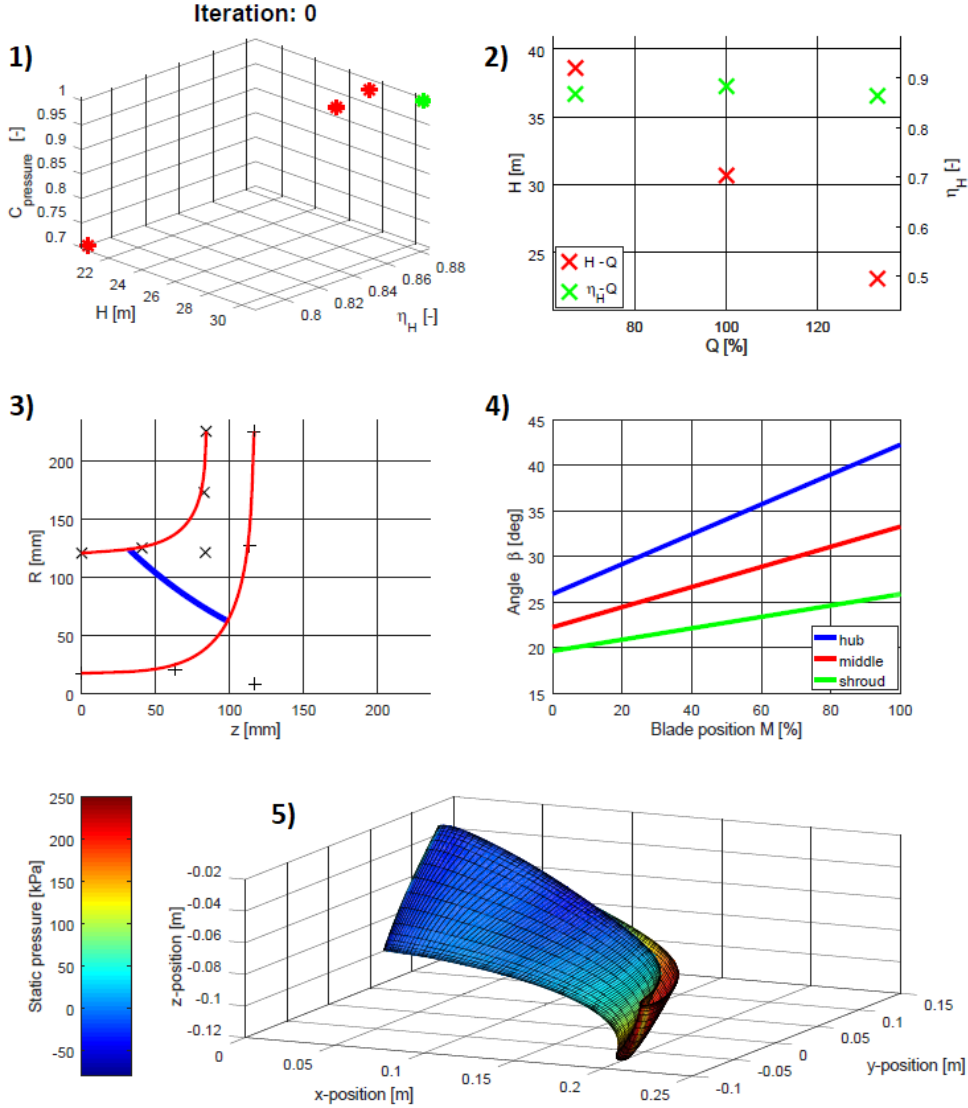
Fig. 3.1: *Software layout.*

Window 1) shows during the optimization procedure the Pareto front with the selected best design (green color). The pareto front consists of the pump head H, the hydraulic efficiency η_H and the operational constant $c_{pressure}$ (all three variables are acquired from the CFD simulations). The best design is established by the evaluation function f defined by eq. 2.1. **Window 2)** outlines two main performance characteristics, namely: $H - Q$ (red color) and $\eta_h - Q$ (green color) in three operation points. These dependencies belong to the current best design. **Window 3)** has a task of presenting the Bézier curves of the pump meridional flow channel (red color) and the leading edge (blue color) of the current best design. **Window 4)** describes the β angle development along the length of the blade. Such development is captured on the three main streamlines - near the hub (blue), near

the shroud (green) and on the middle streamline (red). Plotted β-curves belong to the current best design. **Window 5)** demonstrates the current best shape of the pump blade together with the static pressure distribution.

3.1 Pump turbine

The first main task for the presented optimization software is a problem of finding the proper shape of the **pump turbine** impeller (grant **TH01020982** - *Zefektivnění akumulace energie a zajištění stability rozvodné sítě rozšířením provozního pásma přečerpávacích vodních elektráren*). Such impeller (and the hydraulic machine itself) works in pump and turbine modes, so it must be noted that in the presented thesis the shape optimization was done only for the **pump mode** of the pump turbine.

3.1.1 Requested and given parameters

Requested pump turbine parameters and crucial **optimization parameters** represents table 3.1 [11], [13]. Such table contains values for the prototype impeller and also scaled values for the model impeller, which was measured by **ČKD Blansko Engineering** (ČBE) (section 3.1.4) [11], [13].

Tab. 3.1: *Requested and shape optimization pump turbine parameters* [11], [13].

	Prototype	Model
Pump head H $[m]$	435	34.77
Flow rate Q $[m^3/s]$	26.9	0.181
RPM n $[1/min]$	600	1100

The shape of the pump turbine impeller was also strictly constrained with the dimensional restrictions - table 3.2. Once again, mentioned table 3.2 contains values for the prototype impeller and also scaled values for the model impeller.

Tab. 3.2: *Dimensional constraints* [11], [13].

	Prototype	Model
Inlet diameter d_0 $[mm]$	1560	240.58
Outlet diameter d_2 $[mm]$	2918	450
Inlet width b_0 $[mm]$	670	103.32
Outlet width b_2 $[mm]$	210	32.39
Number of blades z $[-]$	9	9

Presented dimensional constraints firmly set the size of the impeller. This fact means that **size** was **NOT** under the process of the shape optimization. Altogether, **three** impellers were optimized. They are called in following sections: **Design A**, **Design B** and **Design C**.

3.1.2 CFD simulation

The unsteady (URANS) simulations were utilized for the purpose of data correlation between the measurements (section 3.1.4) and CFD simulations. The computational grids of all pump turbine domains such as the distributor (guide vanes), the impeller and the draft tube were built in ICEM CFD and TurboGrid as fully **hexahedral**, only the spiral case (volute) was meshed in ANSYS meshing as **tetrahedral** with the prismatic layers near walls.

SPIRAL CASE (1)

GUIDE VANES (2)

IMPELLER (3)

DRAFT TUBE (4)
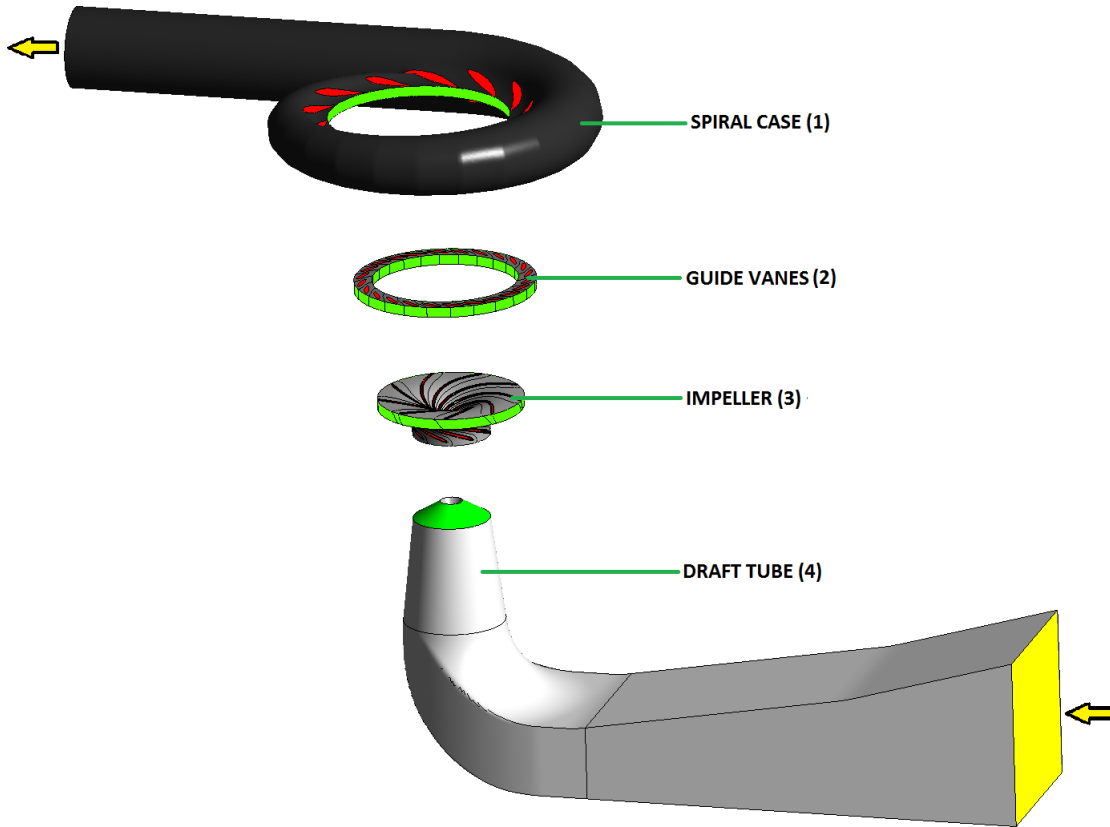
Fig. 3.2: *CFD model of the pump turbine.*

The CFD calculations were done in the commercial software **ANSYS CFX** using standard k-ϵ model of turbulence. The "High Resolution" option was selected for the advection scheme, "Second Order Backward" for the transient scheme and "High Resolution" for turbulence numerics. Chosen time step corresponds to 3° of the pump turbine impeller revolution. Each time step had **5** inner iterations. As a domain initialization served steady simulation (RANS) with mixing planes between relative and absolute computational domains. The requested variables (velocity, pressure, etc.) for the evaluation of the pump head H and the hydraulic efficiency η_H were averaging from the last **10** whole revolutions of the pump impeller. Locations of the pressure taps were identical compared to the measurement performed by ČKD Blansko [11], [13]. For a proper $NPSH_3$ determination, a two-phase calculation (water / vapour) with Rayleigh-Plesset cavitation model with the value of a saturation pressure 3170 Pa (25 ^oC) [15] was utilized. The change of the pump head in $NPSH_3$ determination was inspected over the **6** whole revolutions of the pump turbine impeller.

Complete pump turbine model

The basic pump turbine system consists of four main parts, namely: spiral case (volute) **(1)**, guide vanes (distributor) **(2)**, impeller **(3)** and draft tube **(4)** - fig. 3.2. The RANS and URANS simulations were performed only for the **pump mode**, which is simply described by the yellow arrows in fig. 3.2.

Spiral case (volute)

The spiral case (volute) belongs into a group of absolute computational domains. The tetrahedral mesh with the prismatic layers near the stationary walls was utilized for this domain. The spiral case includes the outlet boundary condition, which was portrayed by a yellow left arrow (fig. 3.2) and characterized by the mass flow rate.

The main performance characteristics were constructed from six operating points $(0.05\ m^3/s \div 0.25\ m^3/s)$, the $NPSH_3$ curve was compiled from three operation points $(0.155\ m^3/s \div 0.195\ m^3/s)$.

Guide vanes

The CFD simulations were performed only for one fixed opening, which had value $a_0 = 20\ mm$. The guide vanes belong to the absolute computational domain, which has two interfaces towards to the spiral case (volute) and the impeller. The fixed blades of the distributor are portrayed by the red color (fig. 3.2).

Pump turbine impeller

All pump impeller designs (A, B, C) were utilized in the relative computational domain. The domain spins with the model RPM ($n = 1100\ 1/min$ - tab. 3.1) and has two domain interfaces (**transient rotor stator**) towards the guide vanes and the draft tube (once again portrayed with the green color in fig. 3.2).

Draft tube

The draft tube (absolute domain) includes the inlet boundary condition portrayed by the zero static relative pressure. This domain also contains the domain interface (green area in fig. 3.2) toward to the impeller and also small portion of the impeller hub, which rotated in the same direction and with same RPM as the impeller.

3.1.3   Complete results and design comparison

Three different geometries of the pump turbine impeller were created as the output of the shape optimization tool based on the Particle swarm optimization, namely: **Design A** (portrayed in this section by the red color) - this design was made in the collaboration with the OFIVK in-house software based on the quasi-potential flow [12], **Design B** (displayed by the blue color) and **Design C** (coloured by green). These designs are compared in following subsections on the geometrical, performance characteristic and the flow patterns base in a way to uncover basic differences and their possible advantages or disadvantages.

Geometrical comparison

First, the geometrical comparison must take place. In fig. 3.3 are all three impeller designs drawn over one another to reveal the main shape and length differences. The red design A is remarkable by the longest blades, on the other hand, blue design B is distinguished by the shortest blade's length. In the middle lies green design C, with the compromisable impeller blade's length.
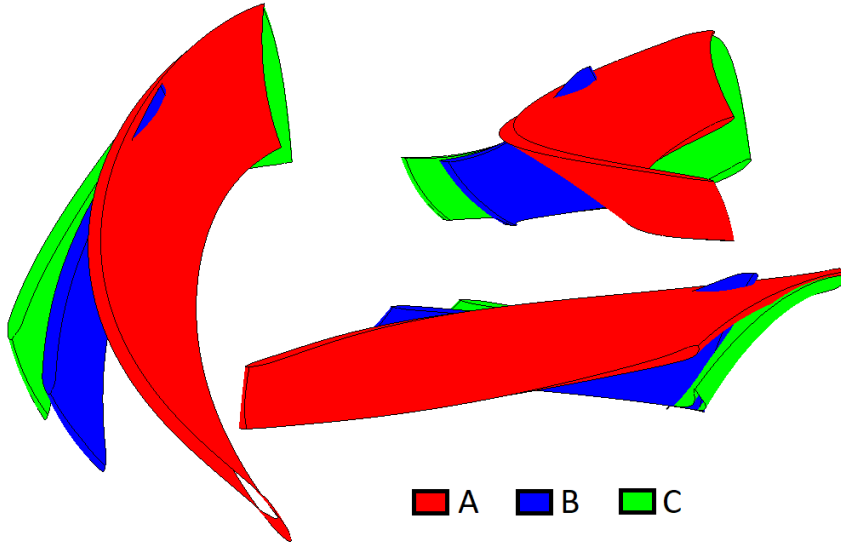
Fig. 3.3: *Design comparison - blade perspective.*

It should be noted that the suitable length of the blade has a key role in a right fluid (water) guiding in the impeller and consequently in the correct behaviour of the pump. This means that the long shaped blades are very convenient for water directing in the pump rotational passages, but the area of blades causes higher hydraulic losses due to greater wall-water interaction and thereby sheer stress. Such losses are one of the main contributors to the pump head and hydraulic efficiency decrease. On the other hand, short blades must deal with a larger "pressure shock" on blade's length compared to the longer blades. With high values of pressure on one side of the blade goes hand in hand low pressure areas on the other side - such areas could initiate the formation of cavitation bubbles.

The last geometrical comparison is focused on the β angle, to be more precise on the inlet and outlet values and the global shape along the blade, which is shown in fig. 3.4. This pump parameter had a crucial part in the proper blade shaping process appearing in the presented shape optimization tool.

As was mentioned, design A was founded on the output from the OFIVK in-house optimization software based on the quasi-potential flow [12]. This design is characteristic with the most complicated shape of the β angle along the blade. The angle near the hub (red color, first figure in fig. 3.4) decreases its value at the beginning (around the leading edge) and afterwards continues almost linearly. On the other hand, β angle in the middle streamline and near shroud could be compared to a quadratic function - a valley-like development with inlet β_1 on one side and outlet β_2 on the other side.
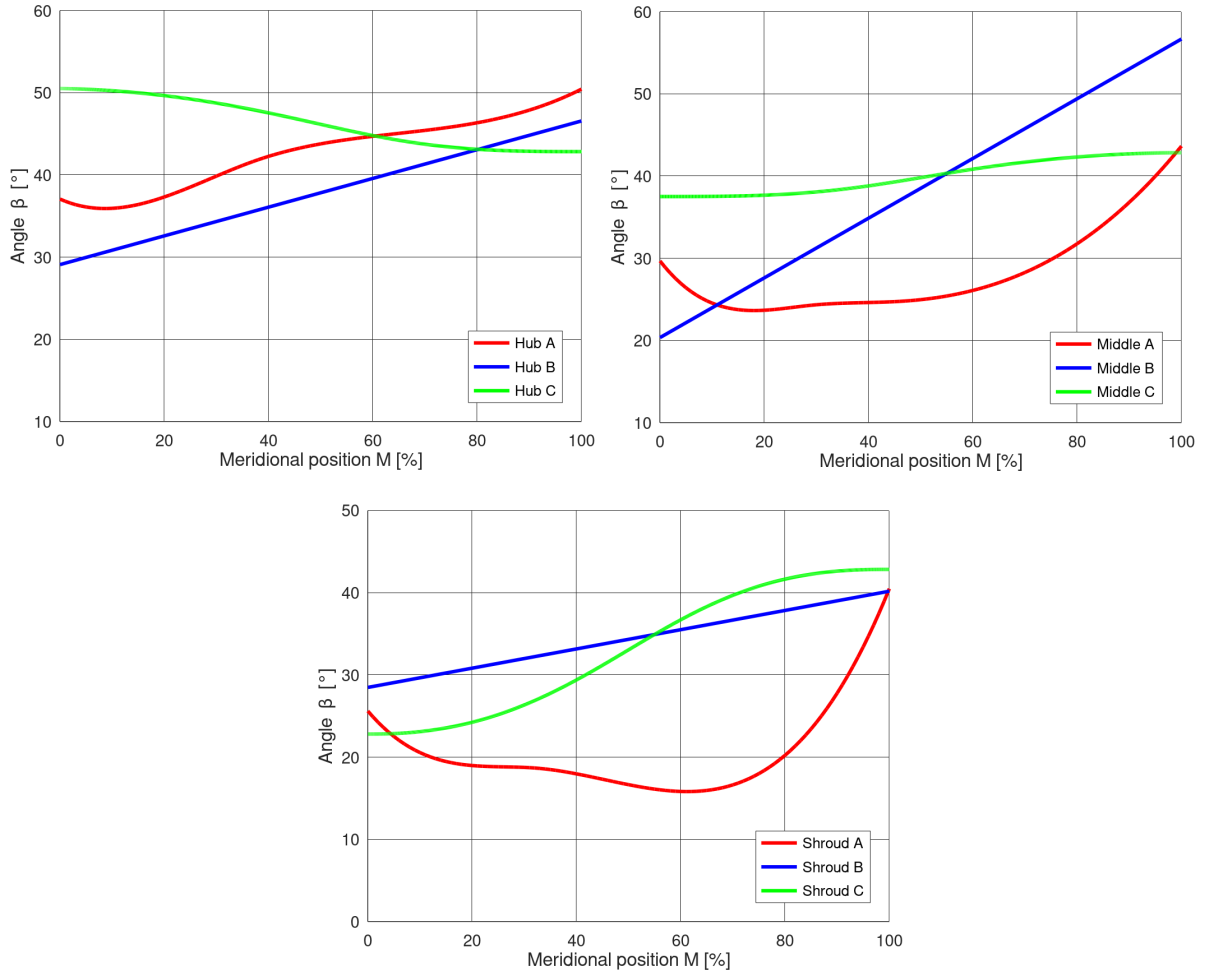
Fig. 3.4: β angle comparison.

Design B explores the pure linear change of the β angle. Such change should be energy efficient with uniform pressure distribution [5].

Design C goes in a way, which was mentioned in Gülich [4]. The β angle development along the length of the blade has the inflection point. This inflection point provides the slow β change at inlet and outlet of the blade, which decreases pressure loading in these locations. Such decrease shows a positive influence on $NPSH_3$ curve [4]. Almost constant β angle near trailing edge is also favourable for impeller trimming.

From the exact value point of view, all impeller designs show quite high values of inlet/outlet β angles - especially outlet β angle, which predominantly lies in interval $20^o - 35^o$ for radial centrifugal pumps [4], [10]. But it must be also mentioned that high values of the outlet β angle are caused by the small magnitude of the outlet width b_2, which has a key role in the determination of β_2.

Performance characteristics and cavitation qualities comparison

Previous subsection brings information about the shapes of optimized impellers, but without a suitable comparison with the main performance characteristic, such as $\eta_H - Q$ or $H - Q$, is quite useless, so and figures 3.5 - 3.7 summarize acquired data from the URANS CFD simulations of the optimized designs A,B and C.
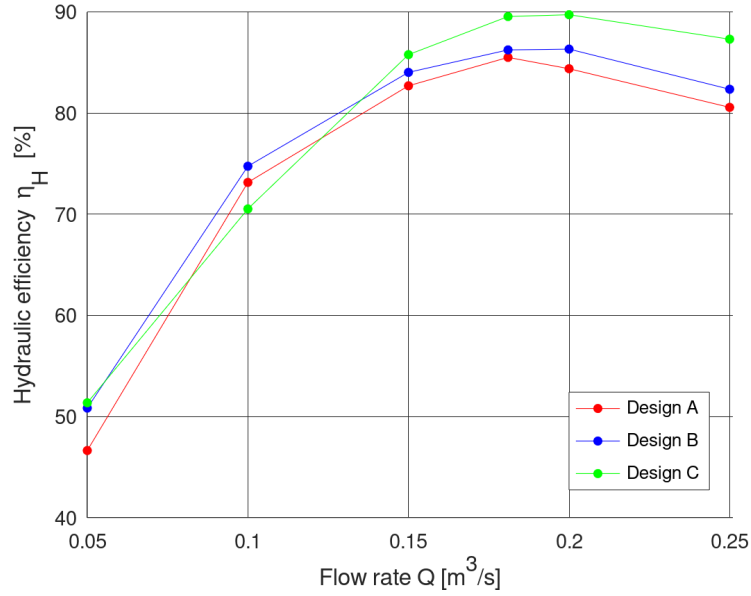
Fig. 3.5: $\eta_H - Q$ *characteristics comparison.*

Unfortunately only **design A** has the highest value of the hydraulic efficiency in the crucial design point characterized by the flow rate $Q = 0.181 \ m^3/s$. Design B and C has the optimum slightly shifted to the right in a way of higher values of the flow rate.
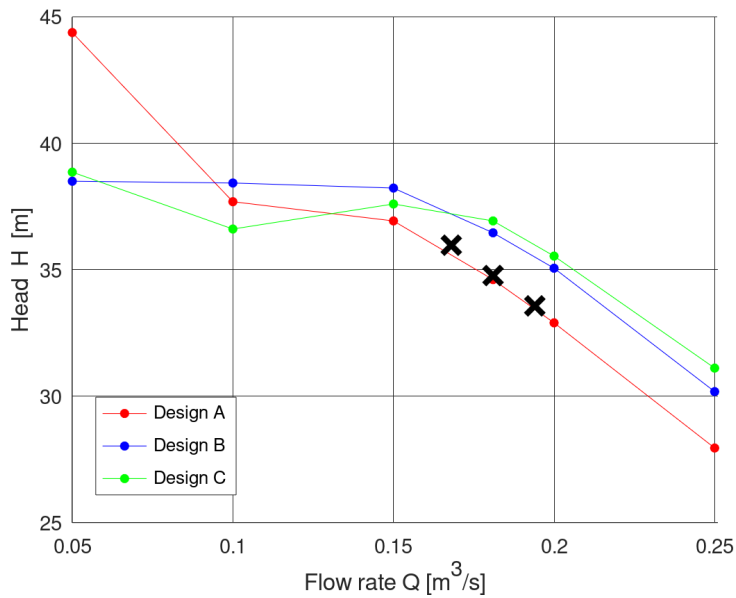
Fig. 3.6: $H - Q$ *characteristics comparison.*

Another important variable, which was closely observed, was the pump head $H \ [m]$. Fig. 3.6 shows comparison between achieved designs and once again all data came from the URANS CFD simulations. In such figure are also marked requested pump head values (portrayed by black crosses) - it is noticeable that only **design A** managed to reach these

values, both design B and design C exceeded e.g. required point defined by the flow rate $Q = 0.181 \ m^3/s$ by 4.41 % and 5.76 %, respectively.

It must be mentioned that the interesting phenomenon was found, while evaluating pump heads, especially in region $Q < 0.15 \ m^3/s$. Usually (without any flow instabilities) head of the centrifugal pump has the highest value in the zero flow rate and with a discharge increase slowly lower its magnitude (when the distributor (guide vanes) is presented mild saddle-like instability is common in regimes with the low value of the flow rate. But the URANS CFD simulations can not detect such "normal" head behaviour towards zero flow rate and huge head overestimations/underestimations are registered. It is possible that the chosen two equation model of turbulence (default k-ϵ in this case) does not properly catch and simulates very turbulent and dissipative flow regimes in complicated flow paths of the pump distributor and impeller, which goes hand in hand with the low values of the flow rate.

The last compared pump characteristic is the $NPSH_3 - Q$ dependency, which has a crucial role in the proper determination of cavitation qualities of the optimized designs - lower the value of the $NPSH_3 \ [m]$ is, then the better performance without cavitation is expected inside the pump turbine system. The most important values of the $NPSH_3$ were examined in three different flow rates, in $Q = 0.155 \ m^3/s$, $Q = 0.181 \ m^3/s$ (optimal flow rate) and $Q = 0.195 \ m^3/s$ (fig. 3.7).
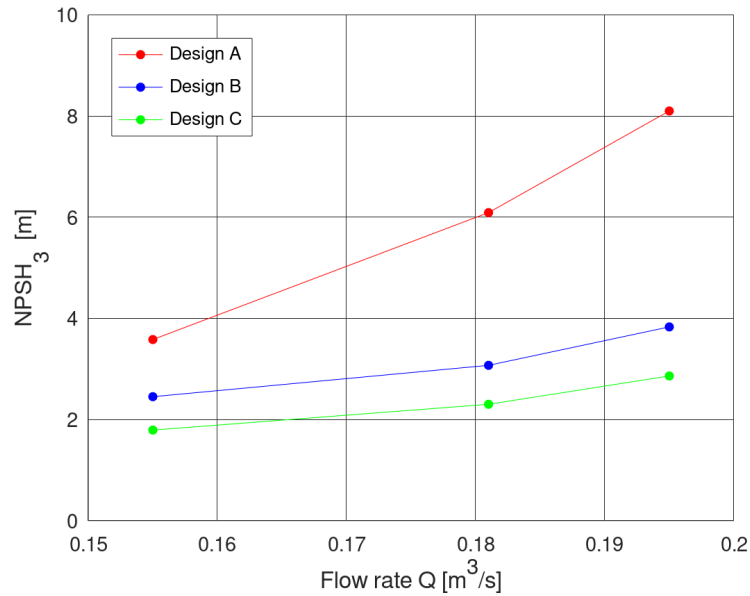
Fig. 3.7: *$NPSH_3 - Q$ characteristics comparison.*

When comparing $NPSH_3$ in optimal flow rate, designs B and C strongly outperformed design A and almost double reduced the value of $NPSH_3$ in such point (from $6 \ m$ to $3 \ m$ in the case of design B and almost to $2 \ m$ in the case of design C - fig. 3.7). Examined points on the left from the optimal flow rate and also on the right are in cases of design B and C below values of design A. Globally, design A shows the worst $NPSH_3$ values in three explored operational points, with minimum shifted towards smaller flow rate and radical $NPSH_3$ increase with discharge $Q = 0.195 \ m^3/s$. On the other hand, **design**

C excels in the $NPSH_3$ field of examination, with the wide range of the lowest achieved values.

3.1.4 ČBE Measurement

Design A was manufactured (fig. 3.8) and subsequently measured in **ČKD Blansko Engineering** (shortly ČBE) in grant collaboration **TH01020982** - *Zefektivnění akumulace energie a zajištění stability rozvodné sítě rozšířením provozního pásma přečerpávacích vodních elektráren.*
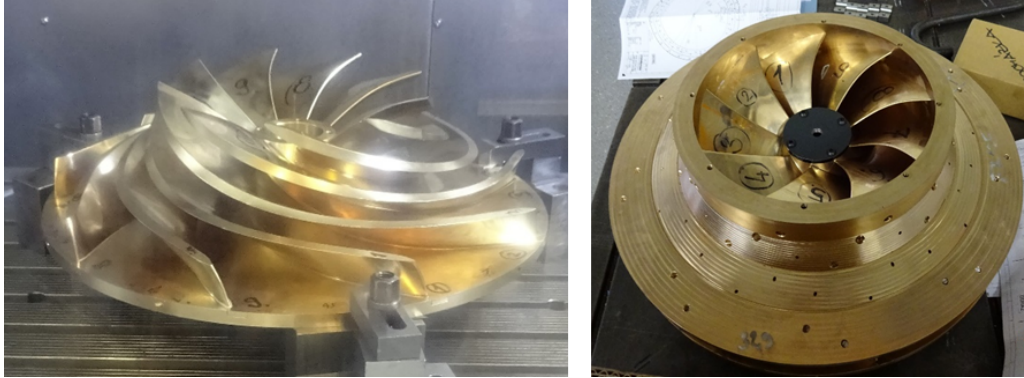
Fig. 3.8: *Impeller model* [13].

Main performance characteristics [13]
Experiments were performed for four different openings of the guide vanes: 18 mm, 20 mm, 22 mm, 24 mm. For comparative CFD simulations was chosen opening $a_0 = 20 \; mm$ (**black** curves in figures 3.9, 3.10 and 3.11).
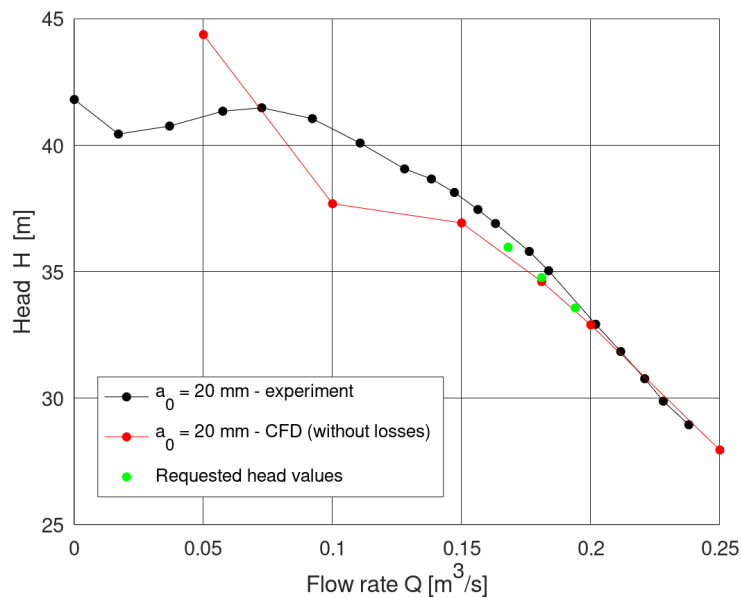
Fig. 3.9: *H-Q dependencies - experiment* [13].
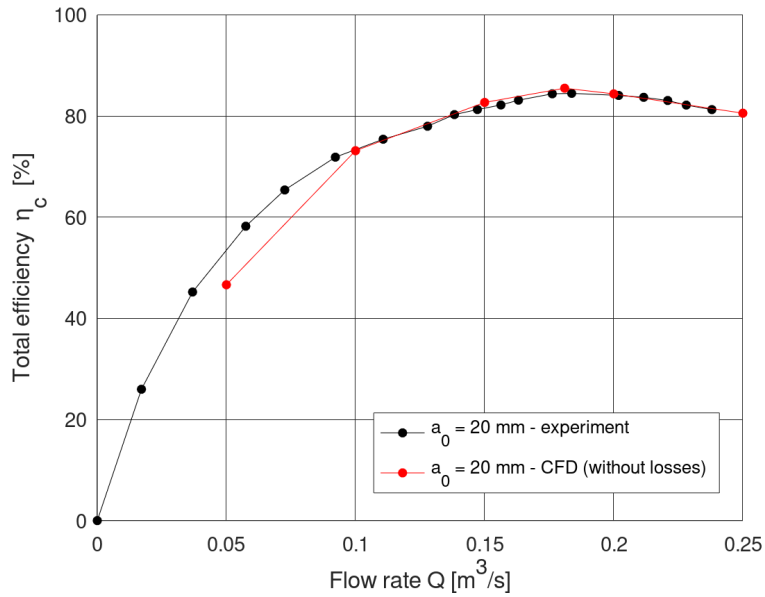
Fig. 3.10: η_c-Q dependencies - experiment [13].

The flow regimes for all openings show instabilities in $H - Q$ dependencies towards to the zero value of flow rate, on the other hand $\eta - Q$ dependencies show wide operation range with high values of efficiency around BEP/requested points. The last main pump characteristic, which was measured and examined by ČBE, was $NPSH_3$ dependency on the pump flow rate (fig 3.11).
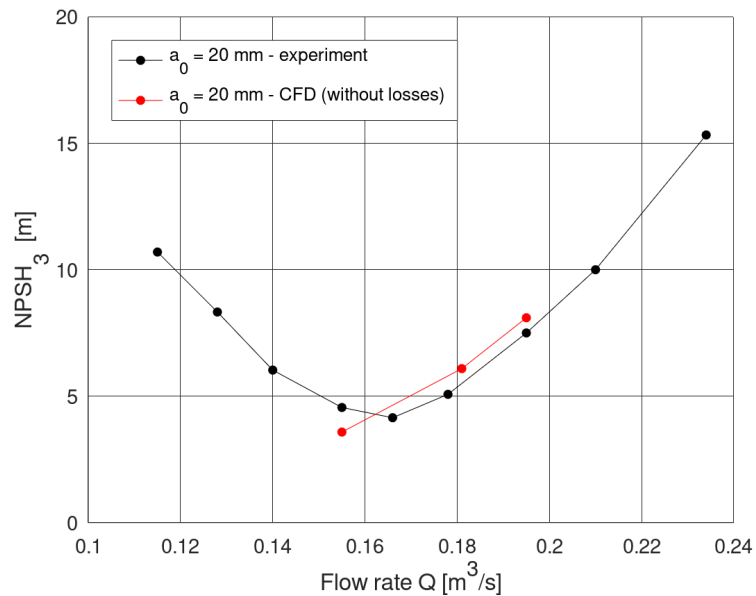
Fig. 3.11: $NPSH_3$-Q dependency - experiment [13].

The $NPSH_3$ curve of the Design A has a common parabolic shape, with the lowest point located to the left from the optimal flow rate, which is characterize by $Q = 0.181\ m^3/s$.

3.2 Low specific speed centrifugal pump

The shape optimization build on the low specific speed pump found in [6], [7].

3.2.1 Requested and given parameters

The main requested low specific pump parameters represents table 3.3.

Tab. 3.3: *Requested pump parameters* [6], [7].

	Prototype
Pump head H $[m]$	32
Flow rate Q $[m^3/s]$	0.00694
RPM n $[1/min]$	1450

Design constraints

The shape and the position of the pump impeller were strictly constrained with the dimensional restrictions united in the table 3.4.

Tab. 3.4: *Dimensional constraints* [6], [7].

	Prototype
Outlet diameter d_2 $[mm]$	320
Outlet width b_2 $[mm]$	10
Number of blades z $[-]$	7

Presented dimensional constraints once again firmly set the size of the pump impeller. This fact means that size was **NOT** under the process of the shape optimization, only the shape was.

3.2.2 CFD simulation

An unsteady (URANS) simulations were utilized for the purpose of data correlation of CFD simulations between presented designs. The computational grids of the low specific speed pump impellers were created in commercial TurboGrid software as fully **hexahedral**. Inlet domain and spiral case were meshed in ANSYS meshing as **tetrahedral** with the high resolution prismatic layers towards the walls.

The CFD calculations were done in commercial software **ANSYS CFX** with identical settings as in subsection 3.1.2. $NPSH_3$ values was **NOT** evaluated in this case.

Complete model

The complete computational domain of the low specific speed centrifugal pump consists of the inlet tube (**1**) (with a certain part of the hub = nut), pump impeller (**2**) and the spiral case/volute (**3**) - all mentioned parts are captured in fig. 3.12.
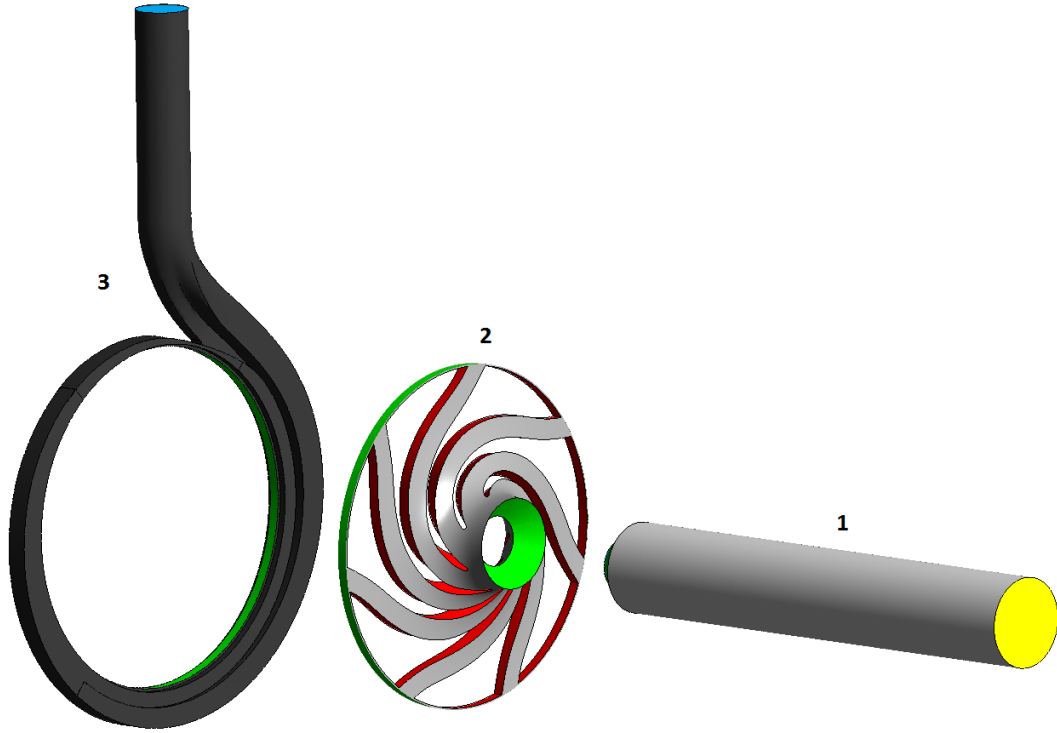
Fig. 3.12: *Complete CFD domain of low specific speed centrifugal pump.*

The inlet tube (**1**) is the absolute non-moving domain, with the nut (part of the hub), which rotated in the same direction and with the same RPM as the impeller. This computational domain contains inlet boundary condition (portrayed by the yellow surface in fig. 3.12), which was characterized by the **zero** relative static pressure.

Spiral case (**3**) is another absolute non-moving domain in the whole computational model. It contains outlet boundary condition, visualized by the blue surface in fig. 3.12. Such boundary condition was defined by the mass flow rate Q_m [kg/s], which was computed using known density of the water $\rho = 997\ kg/m^3$ (this is the default setting in ANSYS CFX commercial software). Total number of the six operational points (OP) was numerically simulated and for the purpose of the mutual comparison also examined ($0.0015\ m^3/s \div 0.01\ m^3/s$)

The last domain is the pump impeller (**2**). It is the relative rotating computational domain with the hub, the shroud and the blades, which rotate with RPM set according the table describing requested parameters (tab. 3.3). Figure 3.12 also includes green surfaces - they are domain interfaces between stationary and rotating parts of the complete pump computational model (for unsteady simulations are in ANSYS CFX called the transient rotor-stator type of the interfaces).

It must be noted that only **one** impeller design was created (optimized) using only the linear change of β angle, mainly because the unsuitable and the unstable tool behaviour during its run, while exploiting the inflection point approach $\rightarrow$ the optimization tool cyclically frozen in the phase of the random generation of the impellers; it cannot create suitable design, which could be afterwards examined via the numerical simulation. Such unstable behaviour is most likely caused by the long and narrow shape of the meridional

flow passage of the pump, where even small changes of the β angle significantly change (deform) the blades. From this perspective, such created impeller is called in following sections the **Optimized impeller** and is compared with so-called **Original impeller** (with thick trailing edges and narrow flow channels), which was designed at OFIVK [6], [7]. The comparison is done only on the CFD simulations base.

3.2.3   Optimized design and complete results comparison

Following section of the text will briefly summarize achieved results of the shape optimization tool, while comparing it with pump impeller described in [6], [7].

Blades of the optimized impeller (design)

Figure 3.13 introduces the optimized design by using two different views - the top and side look.
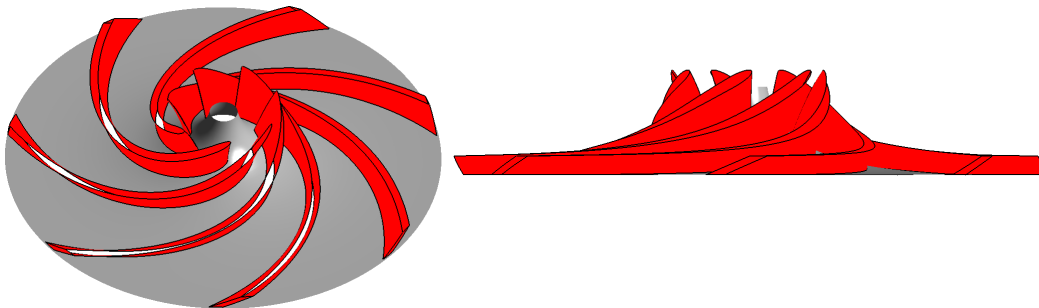
Fig. 3.13: *Geometry of the optimized impeller.*

The optimized design is characteristic for its blade length, the mild curvature of the leading edge and the sloped trailing edge.
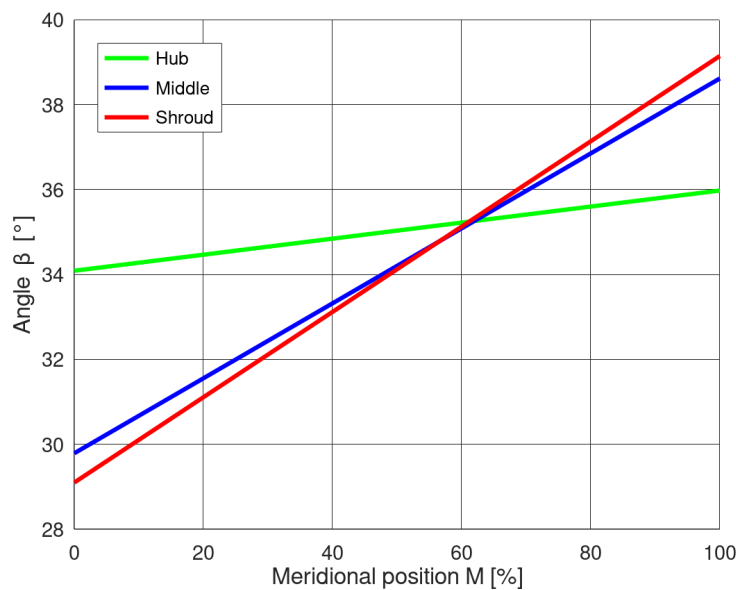
Fig. 3.14: *Developments of the β angle of the optimized impeller.*

Figure 3.14 outlines the β angle development along the length of the blade. The inlet angles are sorted by the values in the descending order from the hub to the shroud. The outlet angles are the other way around, with the highest angle magnitude near the shroud and the lowest near the hub. Interestingly, all the β angle shapes (developments) intersect in 60 % of the blade length.

The higher difference between the β_1 values (especially while comparing values near the hub and on the middle streamline) creates the slight curvature along the length of the blade.

Blades comparison

The original and the optimized impeller of the low specific speed centrifugal pump could be compared from the geometrical point of view. This fact is done in a well arranged way in fig. 3.15, where on the left with the green color are characterized thick blades of the original design and on the right are blades designed by the MOPSO algorithm, which was employed in the shape optimization tool.
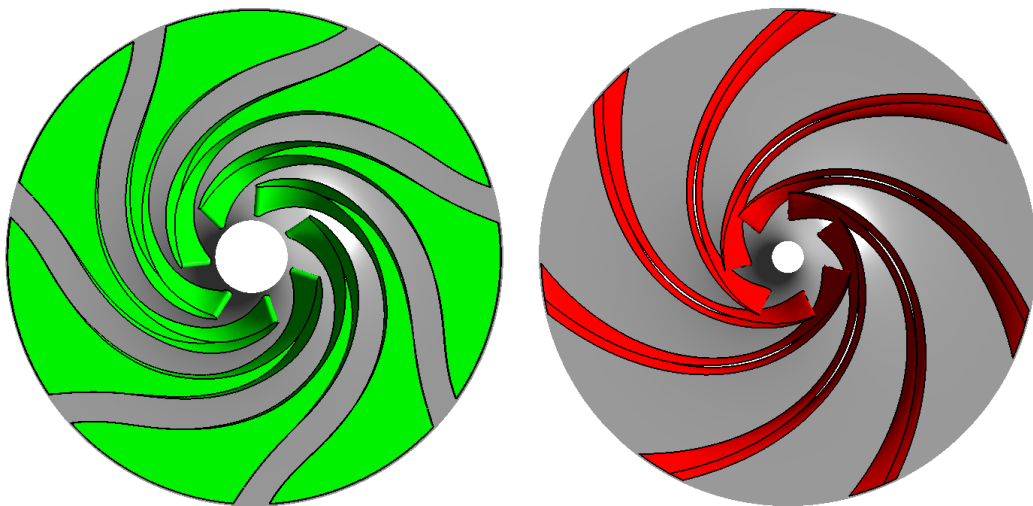
Fig. 3.15: *Design comparison.*

From such perspective (view in fig. 3.15), it is strongly noticeable a crucial geometrical difference between those two impellers. The original design has thick blades especially towards the trailing edge to ensure narrow flow channels, which should better guide water in the small flow rates. The optimized design exploited the traditional blade modelling with the constant blade thickness, which was set to $\Delta = 6 \; mm$ (according to [4]).

Performance characteristics

First performance characteristic is the $H - Q$ dependency (fig. 3.16), with the design point marked as a black cross. From the chosen numerical simulation point of view, the original design did not reach requested head $H = 32 \; m$. On the other hand, the optimized design strongly overestimated required head in flow rate $Q = 0.00694 \; m^3/s$.
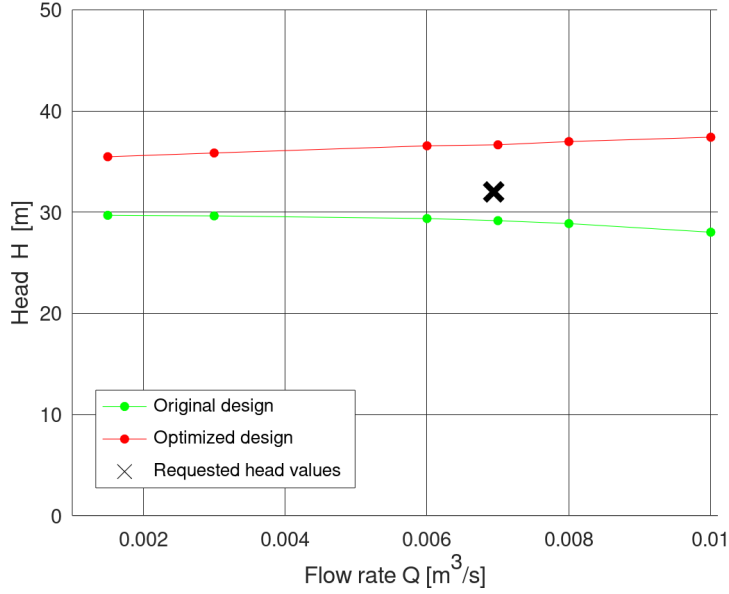
Fig. 3.16: $H - Q$ *dependency comparison.*

The head values have a rising tendency from the smaller flow rates to the higher magnitudes - this fact is quite unusual for the $H - Q$ dependency in the radial centrifugal field of area with the outlet angle $\beta_2 \approx 40^o$. It is the head instability, probably caused by the very dissipative and turbulent flow inside the impeller and the spiral case, thanks to the global small flow rates, which are characteristic for the low specific speed pumps.
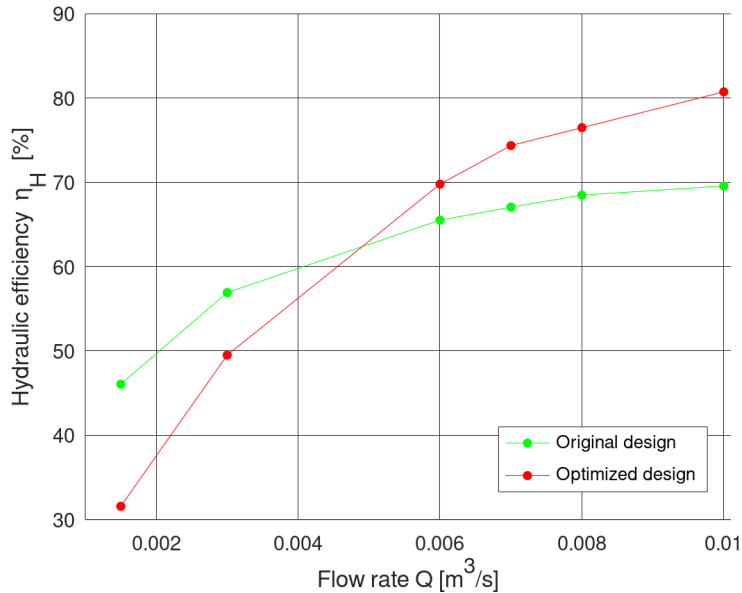
Fig. 3.17: $\eta_H - Q$ *dependency comparison.*

The second evaluated performance characteristic is the $\eta_H - Q$ dependency - fig. 3.17. Both designs do not have the highest possible value of the hydraulic efficiency in the design point defined by the flow rate $Q = 0.00694 \ m^3/s$ - maxima are shifted towards larger

flow rates, where the optimized impeller excels with the higher efficiency magnitudes.

Total pressure and torque pulsation

The pressure pulsations of the optimized (red color) and the original design (green color) are outlined in fig. 3.18, where the pressure difference between the outlet and inlet boundary conditions are depicted (optimal flow rate).
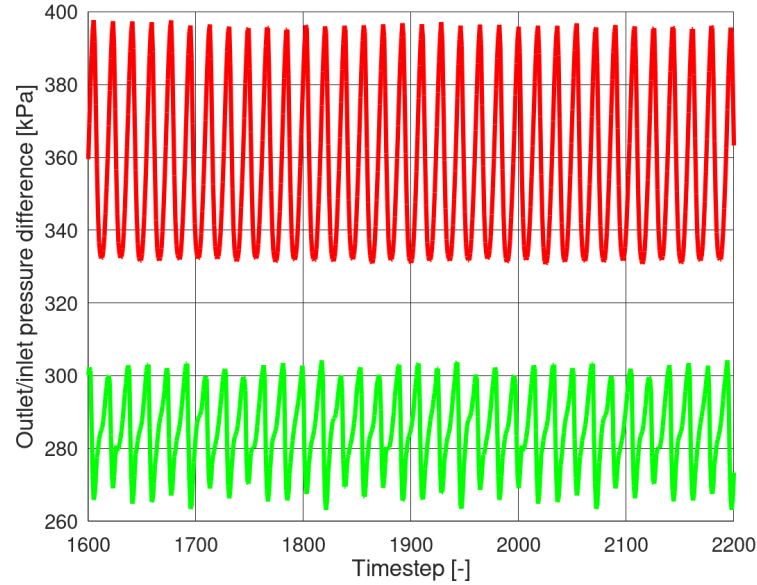
Fig. 3.18: *Total pressure pulsation comparison.*

The optimized design has in certain time passages almost $1.6{\cdot}10^5\ Pa$ pressure difference compared to $0.4 \cdot 10^5\ Pa$ pressure difference delivered by the original design. This fact negatively influenced pump head characteristic, with the strongly inconsistent deliver of the pump head values along the examined time period.
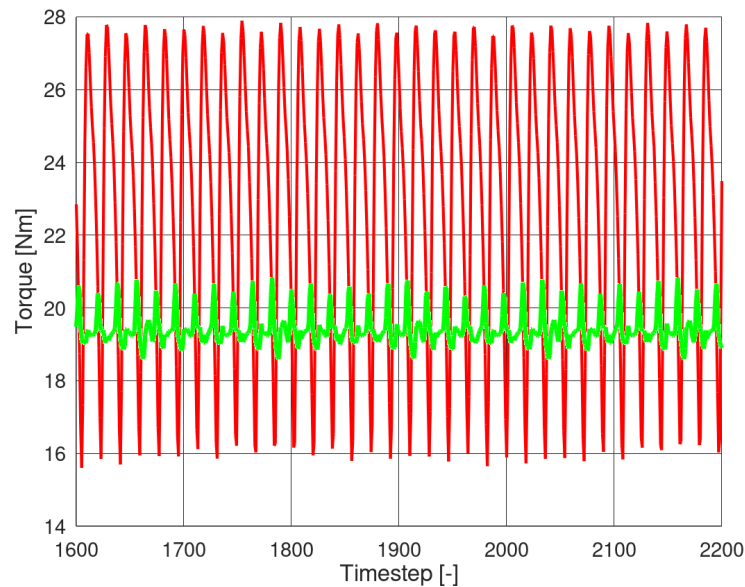
Fig. 3.19: *Torque comparison.*

With the formation of the local eddies in the flow passages of the pump goes hand in hand the pulsation of the examined torque, which consists of the torque from the pump blade, the shroud and the hub. Figure 3.19 compares the torque data of the green original and the red optimized design in the optimal flow rate - the optimized design shows the major periodical torque pulsation with the higher differences than the original design. This phenomenon had the lead role in the strong value inconsistency of the hydraulic efficiency during examined time period, which led even to non-physical values of such examined variable.

Recirculation passages

The crucial fault of the low specific speed centrifugal pumps is the formation of the local eddies, mainly due to the globally small values of the flow rate, which are strongly characteristic for this pump type area. Figure 3.20 focuses and afterwards displays mentioned local eddies inside the flow channels of both, the original an the optimized design, with 3D streamlines and pink isosurfaces of the small values of the velocity. In the case of the original impeller, the recirculation passages formed near the leading edges of the blades, on the other hand, the optimized design shows the local eddies further inside the pump's flow channel. While comparing both mentioned figures, an idea behind the design with the thick blades is strongly noticeable - such blades try to "copy" positions of the created local eddies, presented in the optimized design for the purpose of the unproblematic water flow along the length of the blades.
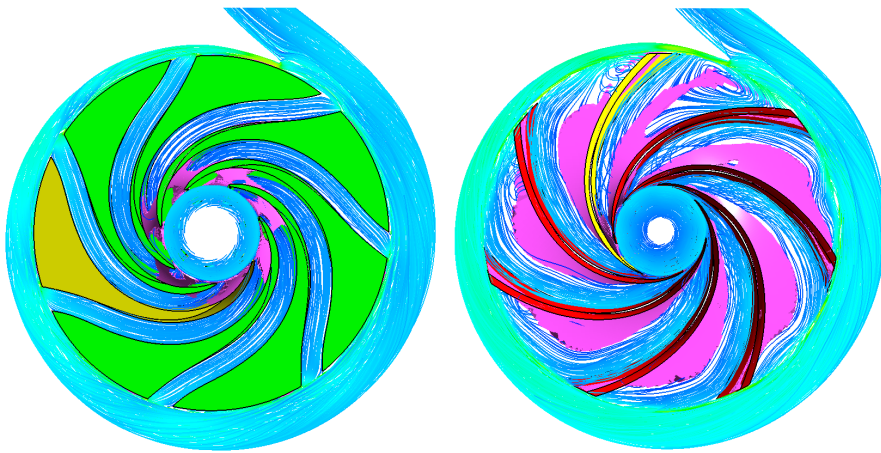
Fig. 3.20: *Streamlines inside of the impellers (optimal Q).*

4 CONCLUSION

This doctoral thesis aims to contribute to the study in the field of the shape optimization in the hydraulic machinery, to be more accurate in the field of the shape optimization of the radial centrifugal pumps. The thesis and author's work is focused on the creation of the shape optimization tool based on the **Particle Swarm Optimization** algorithm (PSOA). Such algorithm is strongly influenced by the social behaviour of the miscellaneous animals, such as birds or ants - it means that the algorithm run is population based (stochastic nature). Each individual member of the current population carries the information about the actual design features, the best achieved design so far and the velocity, which helps the member to properly move in the given computational area. PSOA together with the Pareto principles forms a strong alliance, which is suitable for the exploitation in the multi-objective shape optimization → introducing of the **Multi-objective Particle Swarm Optimization** (MOPSO).

The created shape optimization tool extensively exploited the commercial ANSYS software package, which was fully and autonomously controlled and handled by the **master code** - the complex code within the MOPSO algorithm written in the **MATLAB** programming language and compiled using free licensed **GNU Octave** software. For the impeller designs was exploited **BladeGen** tool (software for the pump/turbine model generation), the fully hexahedral mesh with the high cell resolution near walls was created in **TurboGrid** (here lies a tight bond with BladeGen) and pre-/post-processing and CFD RANS simulations were done in **ANSYS CFX**, which excels in the flow capturing inside the rotary hydraulic machines. All mentioned tools and software from the ANSYS family were handled by the text files, which used only one periodical flow channel of the radial pump for the purpose of time saving and run in the **batch mode** = the application run without the graphical interface (software run in the background of the Windows/Linux operating system). It must be noted that all the RANS simulations were performed remotely using the department's computational cluster **KAPLAN**. For this purpose were created the **shell scripts**, which had the task of the securing the mutual communication and the data transfer between the local PC with the master code and a disk space located in the presence of the KAPLAN cluster.

The crucial development of the shape optimization tool has been supported by three scientific articles, which laid a proper foundation to this academic task:

- MORAVEC, Prokop and Pavel RUDOLF. *Application of a particle swarm optimization for shape optimization in hydraulic machinery.* [8]
- MORAVEC, Prokop and Pavel RUDOLF. *Combination of Particle swarm optimization and Neder-Mead algorithm in diffuser shape optimization.* [9]
- POCHYLÝ, František, RUDOLF, Pavel, ŠTEFAN, David, MORAVEC, Prokop, STEJSKAL, Jiří and Aleš SKOTÁK. *Design of a pump-turbine using a quasi-potential flow approach, mathematical optimization and CFD.* [11]

Two main applications of the shape optimization tool are investigated - the case of the shape optimization of the **pump turbine** impeller and the shape optimization of very **low specific speed pump**. Final results from this optimization were compared with

comparative CFD simulations and in the case of the pump turbine are also compared with the proper measurements performed by ČKD Blansko Engineering (grant **TH01020982** - *Zefektivnění akumulace energie a zajištění stability rozvodné sítě rozšířením provozního pásma přečerpávacích vodních elektráren*).

Pump turbine

Mentioned case of the pump turbine impeller was extensively explored in this thesis, mainly thanks to the creation of three different impeller designs (**design A, B, C**), which heavily differed with β angle modelling approach. The design A, which was strongly influenced by another shape optimization software (based on the quasi-potential flow [12]), was also manufactured as a model and afterwards measured for the purpose of the comparative CFD simulations. Design B explored the pure linear change of the β angle along the length the blade and design C utilized the inflection point within β development to ensure the mild change of the angle near the leading and the trailing edge of the blade. All optimized designs were inspected from several points of view - starting with the main performance characteristics and ending with the flow patterns inside each individual design. It must be noted that not only the one phase URANS simulations were exploited here, but also the two-phase URANS simulation were carefully utilized in the case of the pump turbine to successfully create another type of design comparison $\rightarrow$ the cavitation qualities were extensively explored (but out of the optimization procedure).

Design A has the longest and the most complicated shape of the blade. This development was based on the output from the in-house shape optimization software [12] and set a huge limitation for a possible change - very early stage of the optimization tool worked only in the close surroundings of the initial form of the blade and the distinctive shape change was not an option. Final β angle shape along the length of the blade near the shroud could be compared to the linear change, on the other hand, on the middle streamline and near the hub the β angle shape remotely resembles the quadratic function. Design A has high hydraulic efficiency, but the lowest from all optimized designs. It fulfils requested pump head values (it did not overestimate them as the design B and design C). From the $NPSH_3$ point of view is design A in the end of the line of the optimized impellers with the highest (= the worst) magnitudes in the observed flow regimes. For the next comparison, let's set this design as the **unsuitable** one and compares it with chosen **suitable** design C.

Design B explored the linear change of the β angle on all three examined streamlines. This linear change of the β angle is the simplest one using only the inlet and outlet values of the β angles. Design B is characteristic for the shortest blade length among the all optimized impellers. In all performance characteristics and also in the $NPSH_3 - Q$ dependency lies this design in the middle - between the design A and C. But from a visual point of view this design could **NOT** be recommended due to unnaturally lying and short shape of the blades.

Design C utilized the inflection point in the β angle development mentioned in [4]. Such inflection point was created by the Bézier curves and ensures the gradual change of the β angle at the blade's inlet mainly for the reducing blade loading in such area and also

for the outlet, which could be fully explored in the blade trimming. This design excelled in the hydraulic efficiency point of view, with the highest possible achieved values and with the widest range of the highest efficiency in the requested operational points. Design C also has the lowest values of $NPSH_3$ in the observed flow rates. Where this design falls behind is in the requested pump head magnitudes in the requested flow rates - it overestimated them. Such fact could be corrected by the user/engineer by decreasing the magnitude of the β_2, which is the main contributor in the proper pump head achievement.

So, why is one pump impeller design suitable and another one not? These brief paragraphs will try to show and bring some insight into this subject, while comparing the chosen unsuitable **design A** and the suitable **design C**.

Let's start with the development of the β angle along the length of the blade. From the comparative CFD simulations arises, that the engineer should avoid modelling blades with the extremely crooked shapes of the β angle developments, such as in **design A**. It creates the unstable flow patterns in the flow passages of the radial centrifugal pump, mainly the local eddies near the blades and the sudden static pressure drops inside the flow channel. These mentioned unstable flow phenomena strongly and negatively influence the main performance characteristics of the radial pump. The sudden and radical pressure drops are projected into the $NPSH_3 - Q$ dependency (fig. 3.7) - where design A has the highest (= the worst) values of achieved $NPSH_3$. With the β angle development goes hand in hand the blade loading. From this point of the view, design A has the most unusual blade loading of the all optimized designs - the suction and the pressure side of the blade almost switch their roles near the leading edge, meaning that the suction side had the higher static pressure values than the pressure side and also the overall average static pressure values near leading edge area are lower in the case of the design A, than the rest of the optimized design. On the other hand, the **design C** exploited the approach with the inflection point in the middle of each parametrized streamline. Mentioned inflection points ensured the moderate change of the β angle in the leading edge area and of course in the trailing edge area as well. According to Gülich [4], the mild change in the beginning of the blade will quite positively influence the cavitation attributes of the current impeller - this fact was successfully confirmed by numerical simulations united in fig. 3.7, where the design C came as a winner with the lowest possible $NPSH_3$ values of the all optimized designs. Design C also excels in the highest values and in the widest range of the highest values of the hydraulic efficiency in the requested operational points. One defect of this impeller is that it overestimated requested heads in chosen flow rate regimes, but it could be improved by the engineer by the slight outlet β angle decrease. The important conclusion comes from the perspective of the proper modelling of the β angle - it is crucial to avoid extremely crooked shapes. A way of the simple shapes is a key, but it is very important to make a mild change of the angle near the leading edge - it reduces some of the blade loading, which is afterwards transformed into the favourable values of $NPSH_3$.

When the suitable β angle development is outlined, then the proper length of the blade must be set as well. Let's quickly employ the design B to this debate too and choose the right length, which will form favourable flow patterns in the radial centrifugal pump impeller. The long shaped blades usually guide water well in the flow passages of the pump, but with the length increase goes hand in hand the increase of the area of blade

$\rightarrow$ higher hydraulic losses due to the greater wall-water interaction. On the other hand, very short blades produce smaller losses, but often must deal with the higher level of the blade loading. The design A possesses the longest length of the blade among all optimized designs - with the maximal value of the θ-angle (wrap angle) equals to 160°; the design B is on the other end of the spectrum with the shortest blades, with the maximal value of the θ-angle equals to 100°. Both, the design A and the design B belong into a group with the unsuitable θ-angles $\rightarrow$ in this case (the pump turbine impeller in the pump mode = the centrifugal radial pump impeller) the proper shape of the impeller should possess the maximal value of the θ-angle from the interval $\langle 100^o, 160^o \rangle$ - preferably from the middle of this interval, such as design B with 120°.

To summarize the previous four paragraphs: from the comparative CFD simulations (and also from the measurements) emerge, that it is crucially recommended to make blades of the radial pump impeller **as simple as possible**. The extremely crooked shapes show the inconvenient flow patterns inside the impeller, which leads to the lower values of the hydraulic efficiency and the higher values of the $NPSH_3$.

Low specific centrifugal pump

The second investigated test case for the presented shape optimization tool was the task of finding the proper shape of the very low specific speed centrifugal pump ($n_s = 33\,min^{-1}$). Such types of the pumps suffer with a lot of unfavourable/unsuitable flow phenomena, namely: the formation of the local eddies, the pressure pulsations or the overall structural vibrations. Several modelling methods emerged in past few years to successfully eliminate these flow instabilities, but in this thesis was pursued the "classical" type of blade shape modelling with constant blade thickness along the length of the blade. It must be noted that the presented shape optimization tool cannot fully exploit its great potential here, meaning that the inflection approach in β angle modelling was not used $\rightarrow$ the tool struggled with the initial random impeller creation, mainly due to the uncharacteristic shape of the meridional flow channel of the very low specific speed centrifugal pump.

The optimized design is characteristic for its excessive blade length, the mild curvature of the leading edge and the sloped trailing edge. The impeller possesses the constant blade thickness along the length of the blade - $\Delta = 6\,mm$. The inlet β angles are sorted by the values in the descending order from the hub to the shroud. On the other hand, the β outlet angles are the other way around, with the highest angle magnitude near the shroud and the lowest near the hub. All the β angle developments intersect around 60 % of the blade length.

From the performance characteristic point of view, the optimized design has the overall higher efficiency. The highest value of the hydraulic efficiency is shifted towards the higher values of the flow rate. The optimized design overestimated the requested pump head, which is defined by the value $H = 32\,m$. The shape optimization tool did not manage to eliminate the main flaws of the low specific speed centrifugal pump - in the flow channels of the optimized design are presented noticeable local eddies, which are the main contributors in the pressure pulsation (structural vibrations) and unsuitable (low) values of the hydraulic efficiency. The local eddies were confirmed by the 3D visualisation

of the streamlines inside the pump flow channel, together with the highlighting of the smaller values of the fluid velocity.

The optimized design has significant pressure pulsations. This fact negatively influenced pump head characteristic. With the formation of the local eddies in the flow passages of the pump goes hand in hand the pulsation of the examined torque. The optimized design shows the major periodical torque pulsation with the higher differences than the original design. This phenomenon had the lead role in the strong value inconsistency of the hydraulic efficiency during examined time period, which led even to non-physical values of such examined variables.

The main thesis outcome:

- The successful creation of the shape optimization tool, which in the unique way merged the MOPSO algorithm, the chosen ANSYS software and remote computation on the cluster KAPLAN.
- The confirmation of the suitable properties of the stochastic (population based) optimization algorithm in the hydraulic machinery field of interest.
- The basic outline of the suitable design of the radial centrifugal pump - with the gradual change of the average static pressure in the meridional view; the descending order of β angle inlet values (from the hub to shroud) with the overall simple β angle development or the mild β angle change near the leading an the trailing edge for the purpose of the reducing of the blade loading, which bring the favourable advantage in the cavitation qualities of the current optimized impeller.

LITERATURE

[1] BOWERMAN, R.D. and A.J. ACOSTA. *Effect of the Volute on Performance of a Centrifugal-Pump Impeller.* ASME. 1957. pp. 1057-1069.

[2] COELLO, C.A.C. and M. S. LECHUGA. *MOPSO: A proposal for multiple objective particle swarm optimization..* In Proc. Congr. Evolutionary Computation (CEC'2002), vol. 1, Honolulu, HI, May 2002, pp. 1051–1056 [cit. 2017-04-10]. Available: `http://ieeexplore.ieee.org.ezproxy.lib.vutbr.cz/document/1004388/`.

[3] COELLO, C.A.C., G.T. PULIDO and M.S. LECHUGA. *Handling multiple objectives with particle swarm optimization.* Evolutionary Computation, IEEE Transactions on [online]. USA: IEEE, 2004, 8(3), pp. 256-279 [cit. 2017-04-10]. DOI: 10.1109/TEVC.2004.826067. ISSN 1089778X1089778X. Available: `http://ieeexplore.ieee.org/document/1304847/`.

[4] GÜLICH, Johann Friedrich. *Centrifugal pumps.* 3rd edition. Heidelberg: Springer, 2014, xli, p. 1116. ISBN 978-3-642-40113-8.

[5] HALUZA, Miloslav. *Tekutinové stroje I.* Lectures notes. Brno: University of Technology. Faculty of mechanical engineering. 2013.

[6] KLAS, R., F. POCHYLÝ and P. RUDOLF. *Analysis of novel low specific speed pump designs.* IOP Conference Series: Earth and Environmental Science [online]. 2014, 22(1), 012010 [cit. 2017-08-30]. DOI: 10.1088/1755-1315/22/1/012010. ISSN 1755-1307.

[7] KLAS, R., F. POCHYLÝ and P. RUDOLF. *Influence of low-specific speed pump modifications on stability of Y-Q curve.* EPJ Web of Conferences [online]. Les Ulis: EDP Sciences, 2015, 92 [cit. 2017-08-30]. DOI: 10.1051/epjconf/20159202033. ISSN 21016275.

[8] MORAVEC, Prokop and Pavel RUDOLF. *Application of a particle swarm optimization for shape optimization in hydraulic machinery.* In EPJ Web of Conferences. EPJ Web of Conferences. 2017. p. 1-11. ISSN: 2100-014X.

[9] MORAVEC, Prokop and Pavel RUDOLF. *Combination of Particle swarm optimization and Neder-Mead algorithm in diffuser shape optimization.* 2018. Advances in Hydroinformatics. Springer Singapore, Singapore. p. 997-1012. ISBN: 978-981-10-7218-5.

[10] PACIGA, A., STRÝČEK, O. and M. GANČO. *Čerpacia technika.* Bratislava: Alfa Bratislava – SNTL Praha, 1984. p. 224, 63-557-84.

[11] POCHYLÝ, František, RUDOLF, Pavel, ŠTEFAN, David, MORAVEC, Prokop, STEJSKAL, Jiří and Aleš SKOTÁK. *Design of a pump-turbine using a quasi-potential flow approach, mathematical optimization and CFD.* 2018. IAHR KYOTO 2018.

[12] STEJSKAL, J. *Analysis of the velocity and pressure fields of the liquid using curvilinear coordinates.* Brno: University of Technology. Faculty of mechanical engineering. PhD thesis, 2017.

[13] ŠTEFAN, David, MORAVEC, Prokop, RUDOLF, Pavel and František POCHYLÝ. *Tvarová optimalizace oběžného kola reverzní Francisovi turbíny FR125.* Research report. 2018.

[14] THÉVENIN, Dominique and Gábor JANIGA. Optimization and computational fluid dynamics. Berlin: Springer, 2008, xv, p. 293, ISBN 978-3-540-72153-6.

[15] WEXLER, Arnold. Vapor pressure formulation for water in range 0 to 100 C. A revision. Journal of Research of the National Bureau of Standards Section A: Physics and Chemistry [online]. 1976, 80A(5 and 6), 775 [cit. 2018-06-20]. DOI: 10.6028/jres.080A.071. ISSN 0022-4332

ABSTRAKT

Tato práce se zabývá vývojem optimalizačního nástroje, který je založen na metodě Particle swarm optimization a je poté aplikován na dva typy oběžných kol radiálních čerpadel.

ABSTRACT

This thesis deals with the development of a shape optimization tool based on a Particle swarm optimization algorithm, which is then applied to two different problems of two radial pump impellers.

ŽIVOTOPIS

Jméno a příjmení: Prokop Moravec
Narozen: 6. 1. 1989 v Krnově
Adresa: Hošťálkovy 28, 794 01 Česká republika
Tel.: +420 775 417 084
E-mail: Prokop.Moravec@seznam.cz

Historie zaměstnání
2018 – současnost: Centrum Hydraulického Vývoje s.r.o., výzkumný a vývojový pracovník
2014 – 2018: VUT v Brně, technický a pedagogický pracovník
2014: ČKD Blansko Holding, a.s, výzkumný pracovník
2009: Moravia IT, junior test engineer

Vzdělání a kvalifikace
25. 6. 2014 – 2020: VUT (fakulta strojního inženýrství), Brno – Doktorský studijní program: Stroje a zařízení, téma: Optimalizace průtočných částí hydraulických strojů
27. 6. 2012 – 17. 6. 2014: VUT (fakulta strojního inženýrství), Brno – Navazující magisterský studijní program: Fluidní inženýrství
3. 7. 2008 - 2. 11. 2011: VUT (fakulta strojního inženýrství), Brno – Bakalářský studijní program: Matematické inženýrství
1. 9. 2000 - 30. 5. 2008: Gymnázium Krnov

Zahraniční stáže
1. 4. 2017 – 30. 4. 2017: Slovinsko-University of Maribor, Fakulta strojního inženýrství

Akademicko-vědecké články
MORAVEC, P.; RUDOLF, P.: Population-Based Shape Optimization of a Centrifugal Pump Impeller. MM Science Journal. 2020
MORAVEC, P.; RUDOLF, P.: Combination of Particle swarm optimization and Neder-Mead algorithm in diffuser shape optimization. Advances in Hydroinformatics. Springer Singapore. 2018
MORAVEC, P.; RUDOLF, P.: Application of a particle swarm optimization for shape optimization in hydraulic machinery. EPJ Web of Conferences. 2017
MORAVEC, P.; HLINÍK, J.; RUDOLF, P.: Optimization of hydraulic turbine diffuser. EPJ Web of Conferences. 2016

Dovednosti
Jazyky: Čeština (mateřský jazyk) Angličtina (středně pokročilé znalosti – B1) Němčina (základní znalosti – A1)
Software: Octave, Matlab, Python, ICEM CFD, Ansys Fluent, BladeGen, Ansys CFX, TurboGrid, Windows OS, MS Office, Autodesk Inventor, SolidWorks, FreeCAD